



Perforation location optimization through 1-D mechanical earth model for high-pressure deep formations

Nagham Jasim Al-Ameri¹

Received: 23 August 2021 / Accepted: 21 September 2021 / Published online: 4 October 2021
© The Author(s) 2021

Abstract

Optimum perforation location selection is an important study to improve well production and hence in the reservoir development process, especially for unconventional high-pressure formations such as the formations under study. Reservoir geomechanics is one of the key factors to find optimal perforation location. This study aims to detect optimum perforation location by investigating the changes in geomechanical properties and wellbore stress for high-pressure formations and studying the difference in different stress type behaviors between normal and abnormal formations. The calculations are achieved by building one-dimensional mechanical earth model using the data of four deep abnormal wells located in Southern Iraqi oil fields. The magnitude of different stress types and geomechanical properties was estimated from well-log data using the Techlog software. The directions of the horizontal stresses are determined in the current wells utilizing image-log formation micro-imager (FMI) and caliper logs. The results in terms of rock mechanical properties showed a reduction in Poisson's ratio, Young modulus, and bulk modulus near the high-pressure zones as compared to normal pressure zones because of the presence of anhydrite, salt cycles, and shales. Low maximum and minimum horizontal stress values are also observed in high-pressure zones as compared to normal pressure zones indicating the effects of geomechanical properties on horizontal stress estimation. Around the wellbore of the studied wells, formation breakouts are the most expected situation according to the results of the wellbore stress state (effective vertical stress (σ_{zz}) > effective tangential stress ($\sigma_{\theta\theta}$) > effective radial stress (σ_{rr})).

Keywords Mechanical earth model · Geomechanical properties · Stress state · Abnormal formations · Deep wells

Introduction

Subsurface rock behaviors, including mechanical properties and stress changes during drilling, can detect many problems, especially when the well passes through high-pressure deep formations. Many authors have mentioned these problems using MEM results (Fjaer et al. 2008; Zhang et al. 2009; Ding 2011; Gholami et al. 2013; Rajabi et al. 2014; Nara et al. 2014; Donald et al. 2015).

Formation stress is characterized using the three principal stresses. While drilling a vertical wellbore, the main vertical stress is parallel to the vertical borehole that carries the weight of the overlying formations. Thus, bulk density for a certain incremental depth can be used effectively to calculate overburden formations. At the same time, pore fluids in

porous media will carry some overlying formation that will introduce the effective pressure law defined as total stress minus the pore pressure (Terzaghi and Peck 1984). In a geological relaxed area, rock behavior can be assumed as a linear elastic material; the magnitude of horizontal stress σ_h can be estimated using the well-known poroelastic theory that relates Poisson's ratio (ν) and effective vertical stress. Otherwise, in a tectonically active area, rock deformations are expected to be more exist and rock strain will add another stress component in an elastic rock (Fjaer et al. 2008).

When drilling the rocks, a distribution in the stress is occurred due to the opened free surface that will not be able to transfer shear stresses. Therefore, the principal stresses at the wellbore wall can be represented as an infinite hollow cylinder. To analyze the initiation of stress changes around the hollow cylinder, the principal stresses are given as (Kirsch 1898):

$$\sigma_r = p_w \quad (1)$$

✉ Nagham Jasim Al-Ameri
naghamjasim@coeng.uobaghdad.edu.iq

¹ Petroleum Engineering Department, University of Baghdad, Baghdad, Iraq

$$\sigma_{\theta}^{\min} = 3\sigma_h - \sigma_H - p_w \quad (2)$$

$$\sigma_z^{\min} = \sigma_v - 2\nu(\sigma_H - \sigma_h) \quad (3)$$

When wellbore failure or breakouts are occurring, the magnitude of stresses is estimated as:

$$\sigma_{rr} = p_w \quad (4)$$

$$\sigma_{\theta\theta}^{\max} = 3\sigma_H - \sigma_h - p_w \quad (5)$$

$$\sigma_{zz}^{\max} = \sigma_v + 2\nu(\sigma_H - \sigma_h) \quad (6)$$

where σ_z , σ_{zz} are effective vertical stress, σ_r , σ_{rr} are effective radial stress, σ_{θ} , $\sigma_{\theta\theta}$ are effective tangential stress, and p_w is wellbore pressure.

The stresses at the wellbore wall are the ones that should be compared against a failure criterion. Fjear et al. (2008) illustrated six stress cases (according to σ_z , σ_{zz} , σ_r , σ_{rr} , σ_{θ} , $\sigma_{\theta\theta}$ comparison) for rock failure to occur with the isotropic and impermeable borehole wall.

Stress distribution around the wellbore is introduced in different forms. The tangential and radial stresses are functions of the wellbore pressure P_w , while the vertical stress is not. Therefore, any change in the wellbore will only influence σ_r and σ_{θ} . The induced breakouts around wellbore are the result of wellbore shear failure and are expected to happen at the point of maximum tangential stress. In contrast, hydraulic or induced fracture as a result of rock tensile failure is expected to occur at the point of minimum tangential stress away from the location of breakout around the wellbore.

One-dimensional mechanical earth model (MEM) is a very useful tool, which presents the changes of both mechanical properties and stress along well depth. For each depth interval, rock geomechanical properties in addition to rock stresses can interpret many problems around the wellbore.

For the studied deep wells, detecting the common problems during penetration of high-pressure formations was made using many tools. Al-Ameri (2015) discussed kick tolerance problem encountered within high-pressure formations using the Maximum Allowable Annular Surface Pressure tool, MAASP. Another study showed the estimated high changes in mechanical properties for these deep wells (Al-Kattan and Al-Ameri 2012). The presence of anhydrite–salt cycles is the main cause of abnormal pore pressure for the studied deep wells as mentioned by Al-Mussawi et al. (2009). The presence of these cycles increases the difficulties of dealing with these deep wells in drilling, production, and development stages. Also, high reservoir pressure of the formations under study causes critical changes in wellbore stresses, and therefore, critical

situations for deciding the adequate production strategy reduce many problems during the well life.

The current work is a case study using real four well data for deep wells passing through different important formations in southern Iraqi deep wells. A comparison has been conducted between normal and abnormal formations based on one-dimensional mechanical earth model (1-D MEM) results around the wellbore. Accurate estimation of different types of stresses around the wellbore and determination of failure criterion is provided as a very important tool to predict the ultimate magnitude of rock strength. Many problems were detected for the studied wells using software output, and candidate layers for setting perforation are introduced.

Geology of the study area

The data of four abnormal deep wells (A, B, C, and D) belonged to four oil fields are putting under focusing in this study. The wells have total depths ranging from 4000 to 6000 m. These wells are passing through many formations such as Ratawi, Yamama, Suliay, Gotnia, and Najmah formations. These formations are considered an important oil reservoirs in the area as well as most formations faced many problems while different well operations. The studied wells lie in the Zubair subzone, which forms the most southern unit of the Mesopotamian zone; it exhibits a uniform structural pattern, evidently determined by some changes in the basement. The prominent N–S trend of its structures continues hundreds of kilometers southward on the Kuwaiti and Saudi Arabian territories. The structures consisting of long, relatively narrow anticlines separated mainly in the east by somewhat broader synclines and combined with parallel or oblique trending, short some isometric anticlines, more rarely structural noses. These structures make the accurate estimation of stress magnitude and direction is a crucial step before the beginning of any operations.

The lithology and thickness of the studied formation are different. Ratawi formation is composed of shales interbedded with limestone. For Yamama formation, limestone is the main unit with distinguished units of shale. Suliay formation is considered as a uniform chalky sequence interbedded with limestone. Gotnia formation consists of anhydrite with shale and limestone. Limestone with beds of shale in some areas is found in Najmah formation. The early mentioned difference in formation lithologies for these formations under study causes a clear difference in formation pressure that is a need to accurate estimation of stress magnitude and direction as well as geomechanical properties along these formations.

The direction of maximum horizontal geo-stress is NNE–SSW in well B using the section from 3500 to 4500 m depth, which agrees with geo-stress that leads to the reservoir anticline structure. In Cretaceous formation (3589.3–3702m), the direction of maximum horizontal geo-stress is NNE–SSW, but in Tertiary formation (4122–4489.3 m), NWW–SEE, N–S, and E–W directions exist, and the NWW–SEE direction is dominant.

Mechanical rock properties

It is well known that mechanical properties can be obtained from petrophysical logs using different correlations, which are consequently used to calculate the magnitude of stresses. These modulus parameters indicate rock strength and rock stability under different conditions. The combined elastic modulus E takes into consideration the effect of both shears G and bulk modulus K_b as:

$$E = \frac{4}{3}G + K_b \quad (7)$$

where G , the shear modulus, is defined as the ratio of shear load to lateral deformation. The bulk modulus K_b indicates bulk compressibility, and it depends on the compressibility of both formation solids and fluids.

$$G = \frac{A\rho_b}{tc^2} \quad (8)$$

where $A = \frac{1-2\nu}{2(1-\nu)}$.

$$E = \frac{1.34 * 10^{10} * \rho_b}{t_c^2} \quad (9)$$

where t_c is the transit time from the sonic log, ρ_b is bulk density. Poisson's ratio, ν , was calculated using measured pore pressure (Drill stem test, DST) and leak-off test (LOT) for fracture pressure and calculated overburden pressure using density logs.

$$\frac{\nu}{1-\nu} = \frac{G_f - G_p}{G_{ov} - G_p} \quad (10)$$

Ather method was used to calculate strength modulus as:

$$\nu = \frac{3K_b - 2G}{6K_b + 2G} \quad (11)$$

Compressional wave velocity V_p was calculated using the sonic log as:

$$t_c = \frac{10^6}{V_p} \quad (12)$$

U gamma-ray log to find clay volume V_{cl} then

$$C_R = \frac{1}{K_b} \quad \text{and} \quad \alpha = 1 - \frac{C_R}{C_B} \quad (13)$$

where C_R and C_B are rock and bulk compressibility, respectively, and α is Biot's coefficient. The uniaxial compressive strength (UCS) has been proposed based on studies in different fields by correlating UCS with different well logs or elastic properties (Chang et al. 2006). We can choose the adequate correlation, which is closer to the field under study to estimate UCS of formation. Such as correlations are:

$$UCS = 0.008EV_{cl} + 0.0045E(1 - V_{cl}) \quad (14)$$

$$UCS = 9.95V_p^{1.21} \quad (15)$$

$$T_i = \frac{0.025UCS}{10^6 C_B} \quad (16)$$

where T_i is the tensile strength of the rock, and finally, the critical wellbore pressure that will produce breakout is:

$$P_{BO} = \frac{1.5\sigma_h - 0.5\sigma_H - 0.5\alpha P_p \left(\frac{1-2\nu}{1-\nu} \right) - 1.732T_i}{1 - 0.5\alpha \left(\frac{1-2\nu}{1-\nu} \right)} \quad (17)$$

Methodology of geomechanical modeling

Finding different stress values is considered in the current study using the Techlog software. The following are the calculation procedure and the output results for the studied wells:

1. Pressure calculations and overburden pressure were obtained using density log data, while pore pressure was obtained using Eaton methods based on well-log data (dipole sonic log).
2. Rock dynamic mechanical properties such as Young modulus E , shear modulus G , Poisson's ratio ν , are calculated and considered in this research using sonic and density log data. Equations (8) and (9) are used to calculate E and G . The calculation results are illustrated in Figs. 2, 3, 4 and 5 for each well.
3. In horizontal stresses, many authors suggest that the magnitude of minimum horizontal stress σ_h can be compared against leak-off test (LOT) data if available (Fjear et al. 2008; Gholami et al. 2013). Vertical stress σ_v (equal to $P_{ov} - P_p$) and horizontal stress σ_h are calculated for each well using Eq. (18).

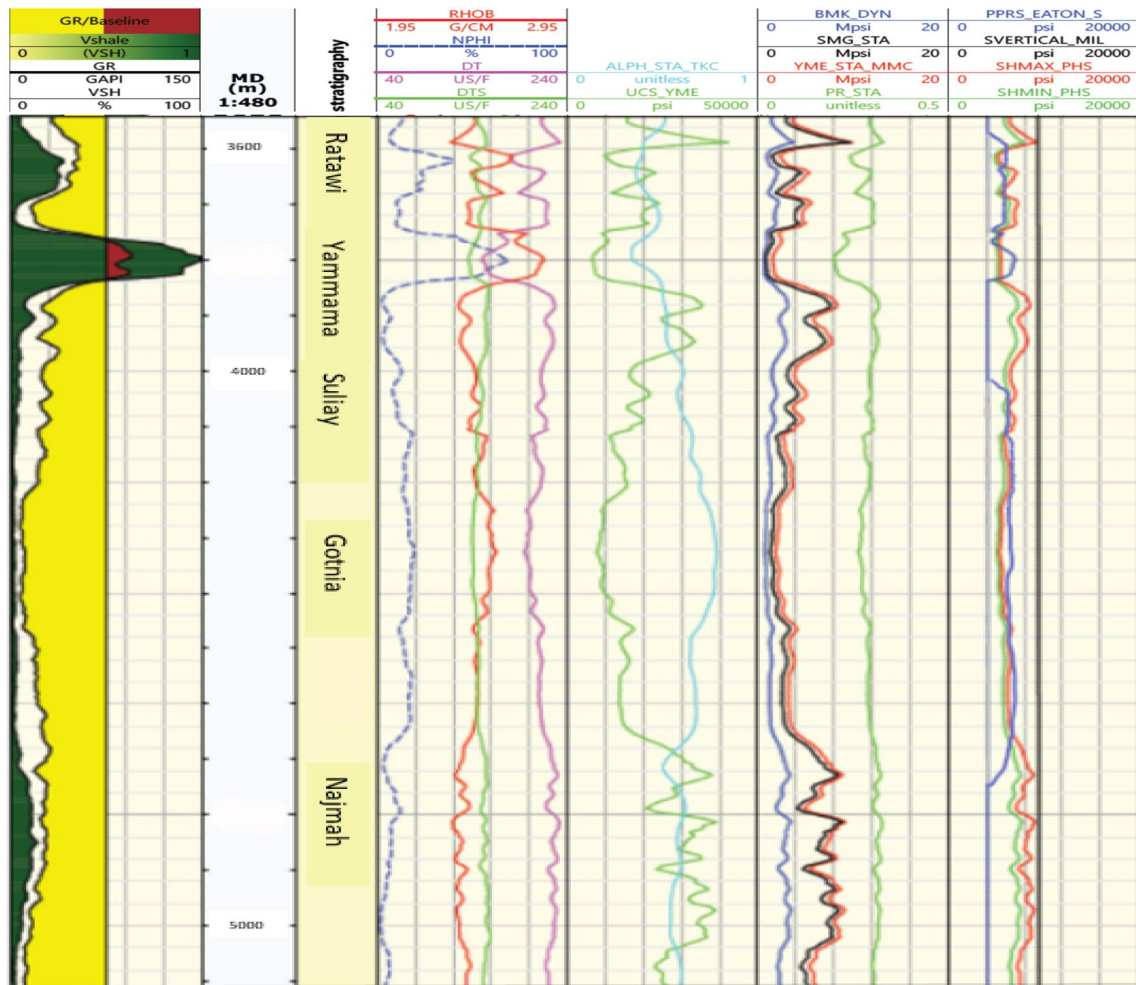


Fig. 2 Calculated mechanical earth model (MEM) for well A

$$\sigma_h = \frac{v}{1-v} \sigma_v - \frac{v}{1-v} \alpha P_p + \alpha P_p + \frac{v}{1-v^2} \epsilon_x + \frac{Ev}{1-v^2} \epsilon_y \tag{18}$$

- The maximum horizontal stress σ_H is calculated using the following equation with all available parameters in that equation, where α is Biot’s coefficient and is calculated using Eq. (19). Strain values are considered equal $\epsilon_x = \epsilon_y$ according to Hubbert and Willis (1957). The calculated σ_v , σ_h , and σ_H are drawn versus depth and presented in Figs. 2, 3, 4 and 5 for each well.

$$\sigma_H = \frac{v}{1-v} \sigma_v - \frac{v}{1-v} \alpha P_p + \alpha P_p + \frac{Ev}{1-v^2} \epsilon_x + \frac{E}{1-v^2} \epsilon_y \tag{19}$$

- Wellbore stresses, after calculating σ_v , σ_h , and σ_H , and the vertical effective stress σ_z and σ_{zz} are calculated using Eqs. (3) and (6) for both induced and breakout

situations. Effective tangential stress σ_θ and $\sigma_{\theta\theta}$ are calculated using Eqs. (2) and (5) for both situations; σ_r and σ_{rr} , the effective radial stresses, are calculated as wellbore pressure. The effective wellbore stresses σ_r , σ_z , σ_θ , σ_{zz} , $\sigma_{\theta\theta}$ are plotted for each well in Figs. 6, 7, 8 and 9.

Results and discussion

The mechanical earth model must be utilized to predict wellbore stresses before drilling operations. Of course, a combined analysis of wellbore stresses and geomechanical properties is the key to minimize wellbore problems or eliminate them.

The vertical stress, σ_v , is the greatest stress in Figs. 2, 3, 4 and 5; this is due to the high depths of the formations under study that is the effect on σ_v calculation to reach 10,000

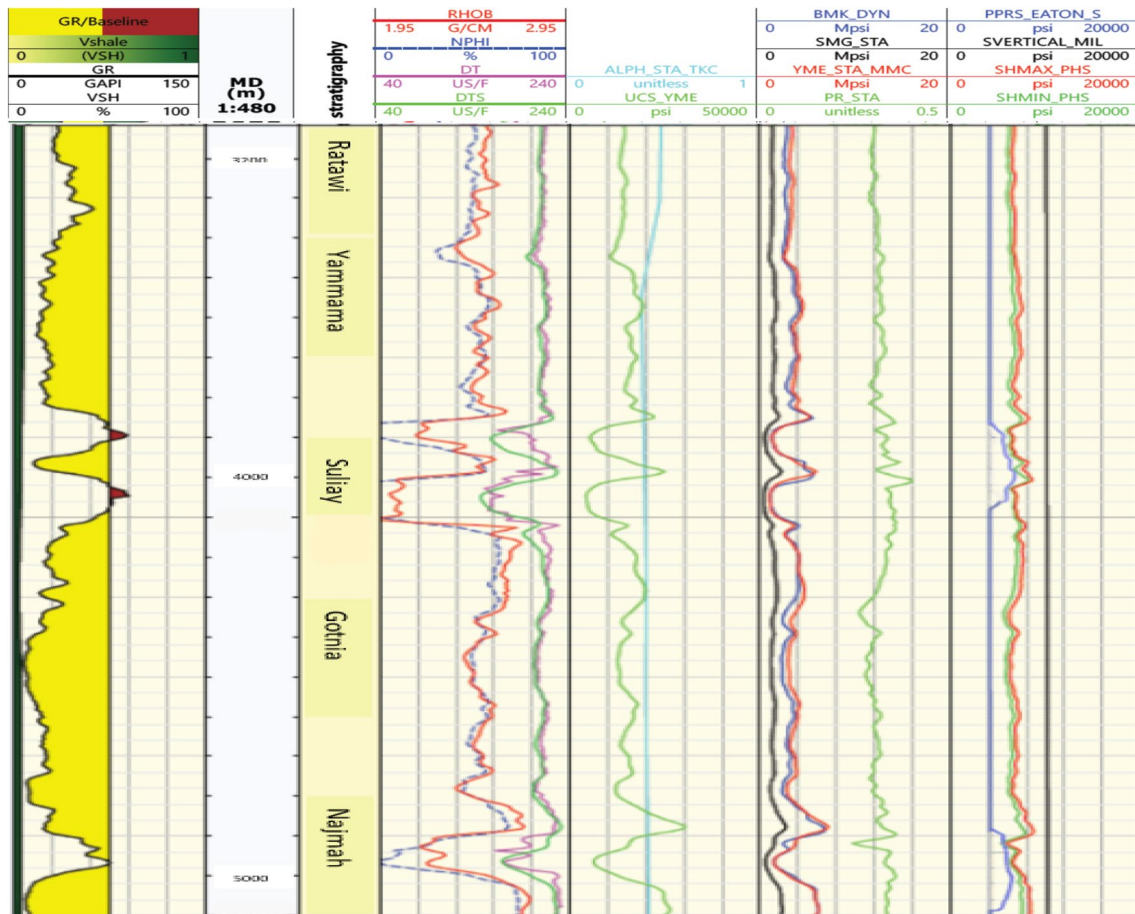


Fig. 3 Calculated mechanical earth model (MEM) for well B

psi for the studied wells. Pore pressure is high in some formations denoting the presence of abnormal formations and is ranged from 4500 to 4900 psi in some intervals within Ratawi, Yamama, Suliay, and Gotnia formations. Searching in the lithological description of current formations under study, it seems that the high pore pressure is caused by the presence of salt anhydrite cycles along these intervals, while pore pressure remained nearly constant as shown in the last track of Figs. 2, 3, 4 and 5 within a range from 4000 to 4500 psi for Najmah formations due to the presence of pure shale intervals in this formation. The presence of abnormal formations can yield many problems such as well kick and if not controlled well blowout. Therefore, equivalent mud density is required to describe the collapse pressure and breakout pressure for these intervals. In general for vertical wells, the reduction of pore pressure in the intervals just below high-pressure formations causes a reduction in rock ability to breakdown and hence fracture pressure decline.

Analyzing different stress types around the wellbore gives an interesting result. In Fig. 6 for well A, the stress situations are $\sigma_{\theta} > \sigma_z > \sigma_r$ and $\sigma_{\theta\theta} > \sigma_{zz} > \sigma_r$ with a regular shape until the region of abnormal pressure arises at 3000 to 4000 m depth

when the stresses are shown a sharp increase with depth; this increase will transform to an equal stresses $\sigma_{\theta} = \sigma_z = \sigma_{\theta\theta} = \sigma_{zz}$ and return to its equal shape when the zone of abnormal pressure disappears. Wells B and C showed the same behavior (with a zone of abnormal ranged from 3500 to 4000 m depth) as illustrated in Fig. 7 for the well B and Fig. 8 for the well C. Well D shows different behaviors as displayed in Fig. 9 where $\sigma_z > \sigma_{\theta} > \sigma_r$ and $\sigma_{zz} > \sigma_{\theta\theta} > \sigma_r$ (the abnormal zone range from 3500 to 4000 m), so it can be concluded that the case of $\sigma_{\theta} > \sigma_z > \sigma_r$ or $\sigma_z > \sigma_{\theta} > \sigma_r$ is the most common state corresponding to borehole breakout. On the other hand, the most common state for borehole fracture $\sigma_r > \sigma_z > \sigma_{\theta}$ did not appear for the studied wells. Borehole collapse will take a place when the wellbore pressure $p_w = \sigma_r$ falls below breakout pressure. These sharp changes in wellbore stresses can cause induced breakouts that result in many problems during penetrating these abnormal formations.

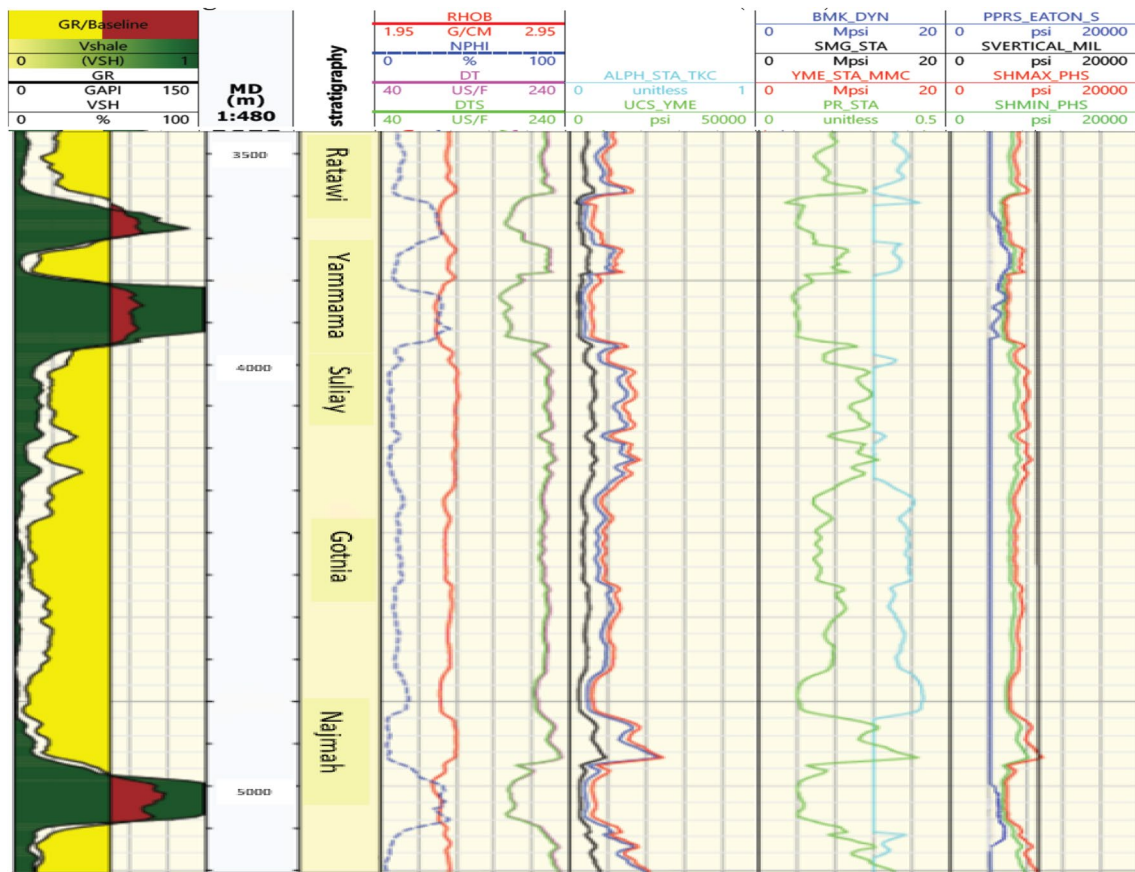


Fig. 4 Calculated mechanical earth model (MEM) for well C

Optimum perforation location

Optimizing the location of perforation improves the drainage area from the reservoir. Perforation location selection depends on the quality of the pay zone along the well. Perforation should be placed at the best petrophysical property area both in terms of storage and in terms of fluid transport. Also, perforation should be placed at better rock mechanical properties in terms of rock ability to initiate fractures; these mechanical properties include minimum horizontal stress, Young's modulus, and Poisson's ratio (Cipolla et al. 2011). In terms of horizontal stress difference ($\sigma_H - \sigma_h$), if high stress variation exists in the area, then perforation location should be selected with a designed cluster distribution so that each perforation cluster should be located at similarly stress locations to promote an equal fluid distribution to the created fractures (Al-Ameri et al. 2020).

In the present work, these crucial conditions for optimum perforation location selection are adopted using 1-D MEM results. These geomechanical parameters were employed to determine the optimum layer position for perforation setting. Good geomechanical quality is mostly represented by high horizontal stress contrast ($\sigma_H - \sigma_h$) and good mechanical

properties represented by low Poisson's ratio, low Young's modulus and low unconfined compressive stress (UCS). The zones of low horizontal stress contrast ($\sigma_H - \sigma_h$), high Young's modulus, high Poisson's ratio and high UCS above or below these selected zones may act as a barrier.

Evaluating the geomechanical quality of the studied high-pressure formations required a careful investigation of the pre-constructed MEM. Careful continuation of the constructed MEM indicates many important requirements to successfully evaluate the formations under study. High horizontal stress difference ($\sigma_H - \sigma_h$) is observed in high-pressure regions. This observation is clear in Figs. 2, 3, 4 and 5 within Najmah formation for the under study four wells in which stress difference ranges from 40 to 60 Mpsi. This high horizontal stress difference makes these regions act as soft formations to induced fractures around the wellbore. The same indication is observed according to geomechanical properties; the zones of high pressure are represented by low Poisson's ratio, low Young modulus, and low unconfined compressive strength (UCS) to give these formations soft indications. Layers with high UCS have high strength against failure, where UCS is weak; it means that the layer has a low range of strength and fracture is easier to occur. Therefore,

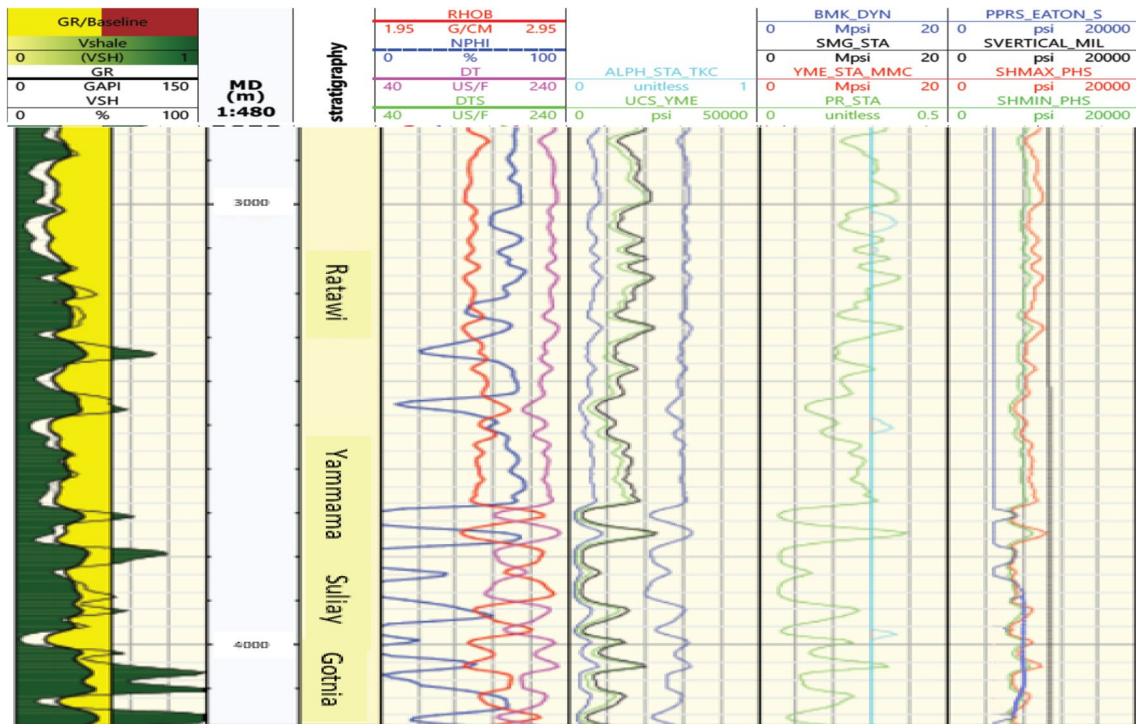


Fig. 5 Calculated mechanical earth model (MEM) for well D

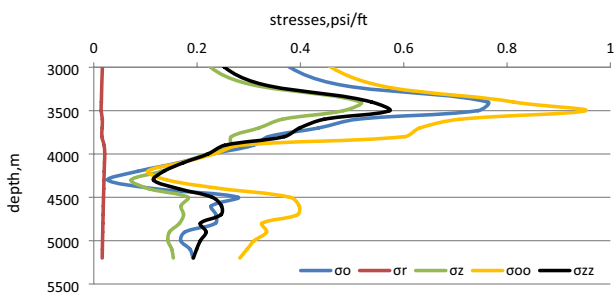


Fig. 6 Different principal stresses versus depth for well A

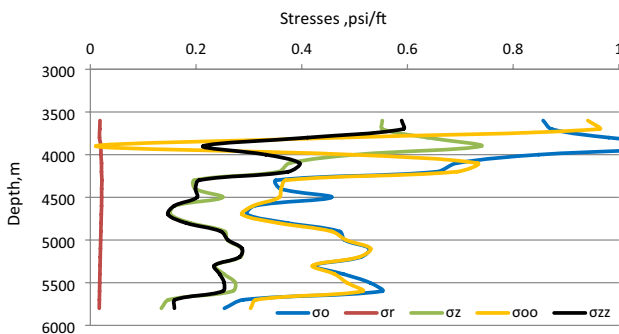


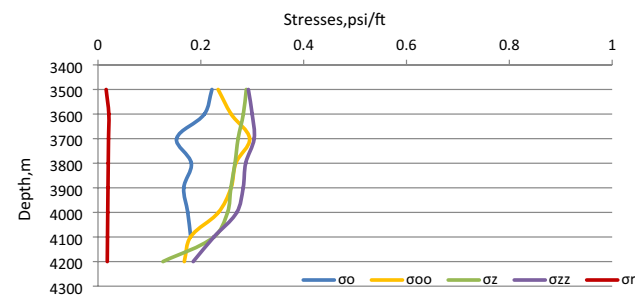
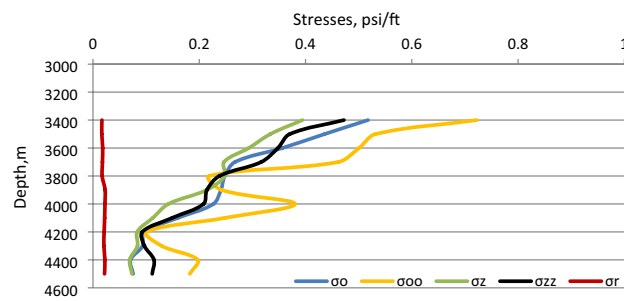
Fig. 7 Different principal stresses versus depth for well B

caution should be taken within these intervals to avoid fluid flow out toward the wellbore as a result of high formation pressures. Lower formation pressure intervals are observed by higher values of Poisson’s ratio, Young modulus, lower stress contrast, and higher unconfined compressive strength such as Yamama formations. In these intervals, it is more difficult to induce breakouts around the wellbore. Young’s modulus controls the elastic response of the formation; it ranges from 2 to 4 Mpsi. An increase in UCS is observed in this formation to reach its maximum value of 25 Mpsi.

Conclusions

This paper focused on the investigating the main wellbore stresses and geomechanical properties for high-pressure reservoirs. The main conclusions that may be constructed from the study results are:

1. Anhydrite–salt cycles besides some shale intervals are the main causes of abnormally high pressure present in the studied formations.
2. Rock mechanical properties such as Poisson’s ratio, Young modulus, and bulk modulus all reduce in the high-pressure zones as compared to normal pressure

Fig. 8 Different principal stresses versus depth for well C**Fig. 9** Different principal stresses versus depth for well D

zones to indicate the presence of anhydrite, salt, and shales.

- Low maximum and minimum horizontal stress values are observed in high-pressure zones as compared to normal pressure zones indicating the effects of geomechanical properties on horizontal stress estimation.
- Lower mechanical properties and horizontal stress magnitude are noticed within shale intervals.
- According to the recorded stress state around the studied wells ($\sigma_z > \sigma_\theta > \sigma_r$ and $\sigma_{zz} > \sigma_{\theta\theta} > \sigma_{rr}$), wellbore breakouts are the most expected situation.
- Yamama and Najmah Formations are the perfect layers for perforation because they provide all the necessary geomechanic conditions to act as productive zone.

Funding No significant financial support has been provided that could have influenced its outcome.

Declarations

Conflict of interest We would like to confirm that there are no known conflicts of interest associated with this publication.

Open Access This article is licensed under a Creative Commons Attribution 4.0 International License, which permits use, sharing, adaptation, distribution and reproduction in any medium or format, as long as you give appropriate credit to the original author(s) and the source, provide a link to the Creative Commons licence, and indicate if changes were made. The images or other third party material in this article are included in the article's Creative Commons licence, unless indicated otherwise in a credit line to the material. If material is not included in the article's Creative Commons licence and your intended use is not permitted by statutory regulation or exceeds the permitted use, you will need to obtain permission directly from the copyright holder. To view a copy of this licence, visit <http://creativecommons.org/licenses/by/4.0/>.

References

- Al-Ameri NJ (2015) Kick tolerance control during well drilling in southern Iraqi deep wells. *Iraqi J Chem Pet Eng* 16:45–52
- Al-Ameri NJ, Hamd-allah S, Abass H. (2020) Investigating geomechanical considerations on suitable layer selection for hydraulically fractured horizontal wells placement in tight reservoirs. In: Abu Dhabi international petroleum exhibition and conference (ADIPEC). <https://doi.org/10.2118/SPE-203249-MS>
- Al-Kattan W, Al-Ameri NJ (2012) Estimation of the rock mechanical properties using conventional log data in north rumaila field. *Iraqi J Chem Pet Eng* 13:27–33
- Al-Mussawi S, Hamed Allah SM, Al-Ameri NJ (2009) Prediction of fracture pressure gradient for deep wells in southern Iraqi oil fields. In: The 6th engineering conference, collage of engineering-university of Baghdad, pp 97–113
- Chang C, Zoback MD, Khaksar A (2006) Empirical relations between rock strength and physical properties in sedimentary rocks. *J Pet Sci Eng* 51:223–237
- Cipolla C, Weng X, Onda H, Nadaraja T, Ganguly U, Malpani R (2011) New algorithms and integrated workflow for tight gas and

- shale completions. In: SPE-146872-MS. <https://doi.org/10.2118/146872-MS>
- Ding DY (2011) Coupled simulation of near wellbore and reservoir models. *J Pet Sci Eng* 76:21–36
- Donald JA, Wielemaker EJ, Karpfinger F, Gomez F, Liang X, Tingay M (2015) Qualifying stress direction from borehole shear sonic anisotropy. In: ARMA, pp 15–364
- Fjaer E, Holt RM, Horsrud P, Raaen AM, Risnes R (2008) Petroleum related rock mechanics, 2nd edn. Elsevier, Amsterdam
- Gholami R, Moradzaden A, Rasouli V, Hanachi J (2013) Practical application of failure criteria in determining safe mud weight window in drilling operations. *J Rock Mech Geotech Eng* 6:13–25
- Hubbert MK, Willis DG (1957) Mechanics of hydraulic fracturing. *Pet Trans AIME* 210:53–63
- Kirsch G (1898) Die theorie der elastizetel und die bedurfnisse der festigkeitslehre. *Z Ver Dtsch Ing* 42(29):797–807
- Nara Y, Kato H, Kaneko K, Matsuki K (2014) Evaluation of principal stress directions and ratio in underground from P-wave velocity measurement in granite. In: ISRM-ARMS8
- Rajabi M, Tingay M, Heidbach O (2014) The present-day stress pattern in the middle east and northern africa and their importance: the world stress map database contains the lowest wellbore information in these petroliferous areas. In: IPTC 17663
- Terzaghi K, Peck RB (1984) Soil mechanics in engineering practice. Wiley, New York
- Tingay M (2008) Borehole breakout and drilling induced fracture analysis from image logs. World stress map project, image logs
- Zhang J, Lang J, Standifird W (2009) Stress, porosity, and failure dependent compressional and shear velocity ratio and its application to wellbore stability. *J Pet Sci Eng* 69:193–202

Publisher's Note Springer Nature remains neutral with regard to jurisdictional claims in published maps and institutional affiliations.